2008년도 한국전기전자재료학회 센서박막재료연구회 및 광주·전남지부 춘계학술대회 논문집 (2008. 04. 17 - 18)

절연층 폴리머의 전하 전송 및 EL 특성

최용성[1], 안성수[1], 김 병철[2], 이경섭[1]
[1]동신대학교, [2]조선이공대학

Charge Transport and Electroluminescence in Insulating Polymers

Yong-Sung Choi[1], Seong-Soo Ahn[1], Byung-Chul Kim[2] and Kyung-Sup Lee[1]
[1]Dongshin University, Chosun College of Science and Technology

Abstract : Polymers submitted to thermo/electrical stress suffer from ageing that can drastically affect their functional behaviour. Understanding the physico/chemical processes at play during ageing and defining transport regimes in which these mechanisms start to be critical is therefore a prime goal to prevent degradation and to develop new formulation or new materials with improved properties. It is thought that a way to define these critical regimes is to investigate under which conditions (in terms of stress parameters) light is generated in the material by electroluminescence (EL). This can happen through impact excitation/ionization involving hot carriers or upon bi-polar charge recombination (a definition that excludes light from partial discharges, which would sign an advanced stage in the degradation process). After a brief review of the EL phenomenology under DC, we introduce a numerical model of charge transport postulating a recombination controlled electroluminescence. The model output is critically evaluated with special emphasize on the comparison between simulated and experimental light emission. Finally, we comment some open questions and perspectives.

Key Words : Thermo/electrical stress, Physico/chemical processes, Charge transport

1. Introduction

Basically, excess energy in insulating materials under thermo-electric stress can dissipate either thermally by emission of phonons and/or optically by emission of photons. Thermal dissipation due to ionic or electronic transport has a positive feedback on the current leading eventually to a thermal runaway when critical conditions with an unbalanced heat supply are reached. This has been discussed at length in textbooks (see for example [1]) and experimental evidence of thermal breakdown has been provided [2]. Thermal runaway however did not give a key to understand electrical ageing, especially in the case of low loss dielectrics like polyethylene based material. For those, current flow is so low that the elevation of temperature due to conduction is usually negligible. Alternatively, excess energy can dissipate - eventually optically - in a range that corresponds to covalent bond energy that is a few eV.

The theory of electroluminescence in large band gap materials predicts different excitation mechanisms depending on the type and distribution of carriers inside the dielectric.

Light can be emitted upon inelastic interactions between mobile carriers (so-called hot carriers with kinetic energy >> thermal energy) and molecules constituting the dielectric. Although structural and chemical changes induced by hot electrons have often been evoked in electrical ageing [3, 4], a clear evidence of their existence in polymeric insulation is still lacking. The other excitation mechanism of EL is encountered when bipolar charge domains spatially interact, leading eventually to radiative charge recombination. This can happen for example when charge promotion occurs via injection from the electrodes, followed by charge transport in the bulk.

We will concentrate on these optical phenomena that are considered as an ageing indicator [5]. Although EL can be excited in insulating materials by any kind of voltage shape of sufficient magnitude, we will restrict our presentation and discussion to the DC case for the sake of simplicity, taken polyethylene as a case study. Although our presentation will be organized by taking the example of polyethylene, one has to emphasize that EL features are largely generic to insulating polymers (except the EL associated with "charge packet" propagation which has only be reported so far in polyethylene and polypropylene).

2. Experimentals

Considering a voltage waveform as shown in Figure 1-a, recording EL shows:

- A transient emission, detected upon rising up the voltage to the targeted level. Its occurrence and persistence depend critically on the field. One example is given in Figure 1-b.
- A continuous emission, stable in time, detected above a material-dependent threshold field (Ec), the later being correlated with a change in the currentvoltage characteristics (as shown in Figure 1-c).
- An oscillatory emission, associated with charge packet propagation, shown in Figure 1-d.
- A transient emission (fast) when grounding the sample, if the sample was polarized in such a way that space charge accumulates. This is shown in Figure 1-e

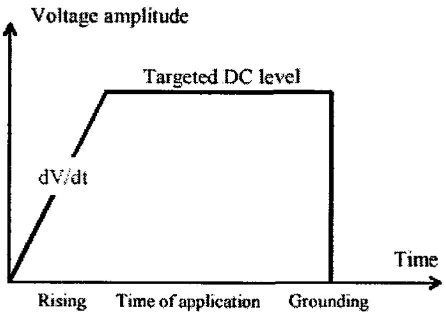

(a) Voltage waveform (grounding means setting the voltage to zero)

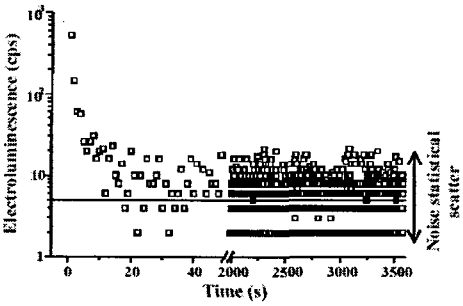

(b) Transient EL upon rising up the voltage (PE, 40 kV/mm, 1 s sampling time)

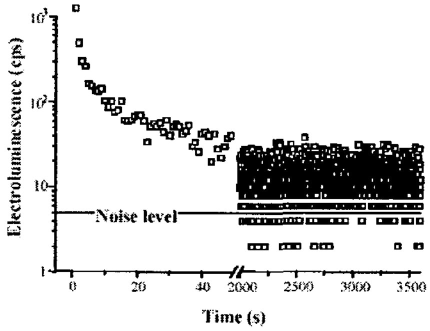

(c) The continuous level is evidenced at long time above the photomultiplier noise level (PE, 80 kV/mm, 1 s sampling time)

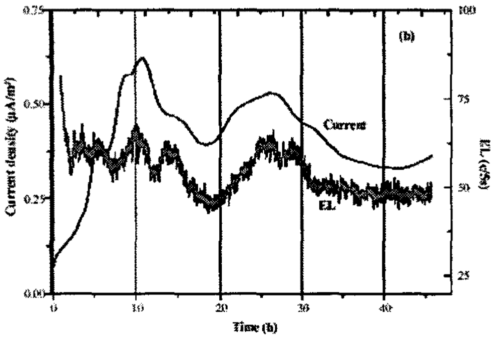

(d) EL and current oscillations during charge packet propagation (PE, 150 kV/mm, 5 s sampling time)

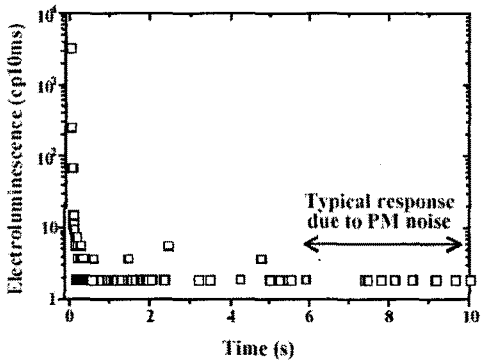

(e) Transient EL upon grounding (PE, 50 kV/mm, 10 ms sampling time)

Fig. 1. Scheme of the different EL phenomena observed in PE under DC voltage application. In Figure b and c, the voltage is applied using a high voltage switch, leading to (uncontrolled) dV/dt << sec

A unique set of parameters was sought for so as to fit all the available experimental measurements (external current, space charge distribution, electroluminescence), for three different experimental protocols. In spite of this very severe requirement, fit between simulation and experiment is good [6]. The parameters that gave the best fit are given in Table 1. It is noteworthy that an initial density of free charges up to 5x10^{-1} C.m^{-3} was set in each case. The charge was supposed to be uniformly distributed throughout the sample and of equal density for positive and negative carriers at each point (zero net charge). This level of charge is assumed to simulate residual charges that are likely to exist in any dielectric, but will not be seen in space charge measurements due to the limited sensitivity of detection techniques (order of 10^{-1} C.m^{-3}), and to the fact that residual charges of a given polarity could be neutralized by an equivalent density of charge with opposite sign, giving a net zero density. The influence on the simulation results of the initial charge density is considered in the next paragraph. It is an important factor to take into account for fitting model and experiments. In the following, we focus on the simulated recombination rate that is directly comparable to the measured EL.

Table 1. Optimized parameterization of the model to fit external current, space charge distribution and electroluminescence at different field levels and for three different experimental protocols in LDPE.

Symbol	value	units
Recombination coefficients		
S_0 trapped electron/trapped hole	4.0 10^{-3}	m^3.C^{-1}.s^{-1}
S_1 mobile electron/trapped hole	4.0 10^{-3}	m^3.C^{-1}.s^{-1}
S_2 trapped electron/mobile hole	4.0 10^{-3}	m^3.C^{-1}.s^{-1}
S_3 mobile electron/mobile hole	0	m^3.C^{-1}.s^{-1}
Trapping coefficients		
B_e electrons	1.0 10^{-1}	s^{-1}
B_h holes	2.0 10^{-1}	s^{-1}
Mobilities		
electrons	1.0 10^{-14}	m^2.V^{-1}.s^{-1}
holes	2.0 10^{-13}	m^2.V^{-1}.s^{-1}
Maximum trap densities		
N_{oet} for electrons	100	C.m^{-3}
N_{oht} for holes	100	C.m^{-3}
Injection barrier heights		
w_{ei} for electrons	1.27	eV
w_{hi} for holes	1.16	eV
Detrapping barrier heights		
w_{tre} for electrons	0.96	eV
w_{trh} for holes	0.99	eV
Initial charge density (net zero)	Up to	
electrons	5.10^{-1}	C.m^{-3}
holes		C.m^{-3}

3. Results and Discussion

Figure 2 shows the recombination rate of mobile electrons with trapped holes as a function of the spatial coordinate x, computed for a field of 60 kV/mm without initial charge density. For short stressing time (<130 s), the recombination rate is null, just because negative and positive carriers do not coexist. Beyond that time, the recombination rate passes through a maximum (t=150 s) and continuously decreases afterwards. The peak corresponding to the maximum recombination rate (for mobile electrons) progressively moves towards the anode for times in the range 130-200 s. A symmetrical situation holds for recombination of mobile holes with trapped electrons in the cathode vicinity. Taken all together, the model forecasts a change in the location of EL during stressing, from the middle of the sample to the regions near both electrodes. Of course, the EL measurement is a space-integrated quantity and the location of the emission in the depth cannot be checked.

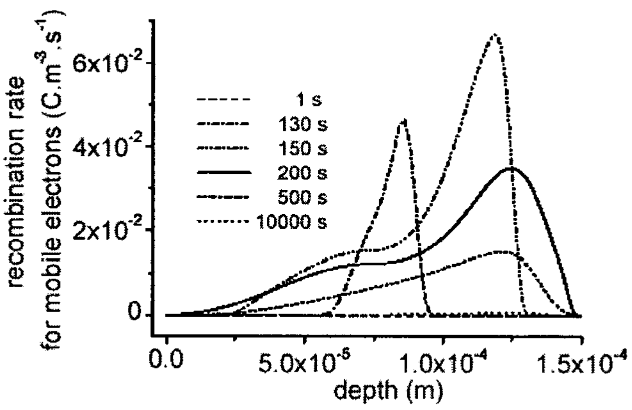

Fig. 2. Recombination rate profiles for mobile electrons/trapped holes as a function of time (cathode on the left, anode on the right, 60 kV/mm field, zero initial charge density). A symmetrical figure (recombination close to the cathode) holds for mobile holes/trapped electrons. Note that the simulation has not been realized with the parameters of Table 1, without consequences on what is discussed here.

The time-dependence of the recombination rate at different fields is shown in Figure 3. It is interesting to note that a recombination-controlled EL model predicts transients EL upon voltage application and upon sample grounding, consistently with the experimental behaviour. In order to compare simulation and experiment, one has to consider the sensitivity limitation of the light detection set-up, that incorporates the photomultiplier characteristics and the solid angle under which is seen the sample by the optical system. However, we are still lacking the radiative efficiency of a single recombination event.

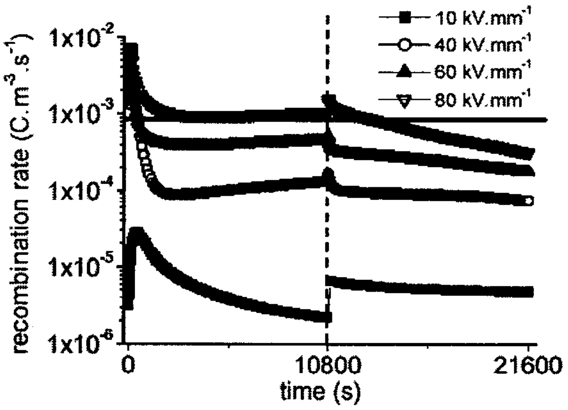

Fig. 3. Time dependence of the recombination rate at different fields in the polarization/depolarization protocols. The full line represents the minimum recombination rate that would give rise to an emission at a detectable level. Initial charge density (net zero) is 10^{-1} C.m^{-3} at 10 kV/mm and $5x10^{-1}$ C.m^{-3} at 40, 60 and 80 kV/mm.

A quantitative derivation of the minimum recombination rate that would be detected as light is therefore out of reach. We therefore take the party to evaluate this minimum rate by considering experimental results. We know from experiments that transient upon voltage application is detected above 40 kV/mm (Fig. 1 b), but there is no transient detected upon grounding at this field level. This means that the minimum detectable rate in Figure 3 has to be located between 2.10^{-4} and 10^{-3} C.m^{-3}.s^{-1}. At 80 kV/mm, both transients are seen and there is a continuous level of light (Fig. 1 c), meaning that the minimum rate in Figure 6 is at about 10^{-3}.C.m^{-}3.s^{-1}. Taking into account the numerical values characterizing the set-up, we derive a radiative efficiency of 10^{-6} for the recombination process.

Retaining this value and plotting the curve in the range of measurement that is accessible by the experiment, we obtain Figure 4 which is consistent with experimental results (semi-quantitatively).

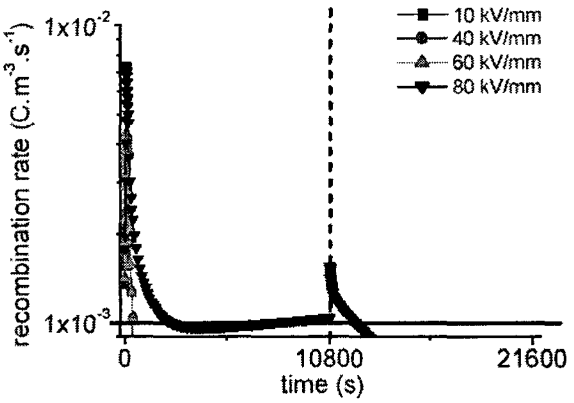

Fig. 4. Time dependence of the recombination rate at different fields, re-plotted with insertion of the minimum level of recombination that would give rise to a detectable EL signal (solid line).

The main discrepancy between simulation and experiment lies in the shape of the transient at voltage application. We have seen that a "pure" recombination controlled EL under the assumption of bipolar injection from the electrodes yields a threshold in time that is not observed experimentally. The presence of initial charge density that is taken into account in the actual simulation can remove the threshold in time, but the transient EL still exhibits a maximum in intensity that is shifted in time (see Figure 4), a feature that is not observed in experiments. For that reason, we think that hot carriers effects should have to be introduced in EL excitation at short time to get a better description of the actual situation.

Figure 5 shows a comparison of the experimental EL and simulated recombination rate taken at the end of each step, i.e. at t = 300 s. We have retained the value of 10-3 C.m-3.s-1 as the minimum value of the recombination rate that would give rise to a detectable EL signal. It can be seen that the fit is extremely good, indicating an onset for the EL at 60 kV/mm. This result gives a considerable support to previous work [5] indicating that the continuous EL observed under DC is the consequence of the formation of bipolar domains near injecting electrodes, transport and subsequent recombination of Transients in the EL signal are detected when increasing the voltage from one step to the next one. Their general characteristic is very close to the one shown in Figure 1 c, namely the EL is max when the step voltage is reached with a decreasing intensity afterwards.

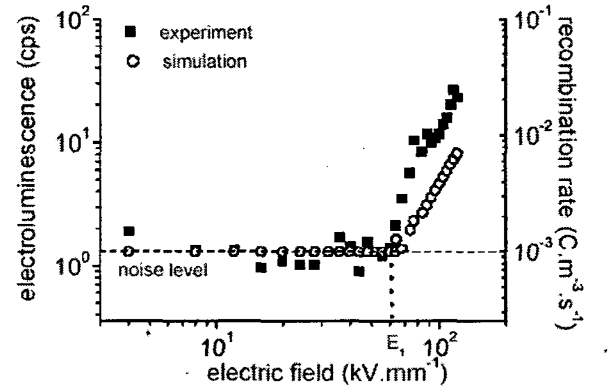

Fig. 5. Comparison of experimental EL and simulated recombination rate.

Simulated recombination rate also shows a transient but the maximum is occurring during the step as shown in Figure 6. It is therefore not possible to fit the shape of the transient using a recombination-controlled EL model.

Again, it appears to be important to take into account hot carrier effects in EL excitation.

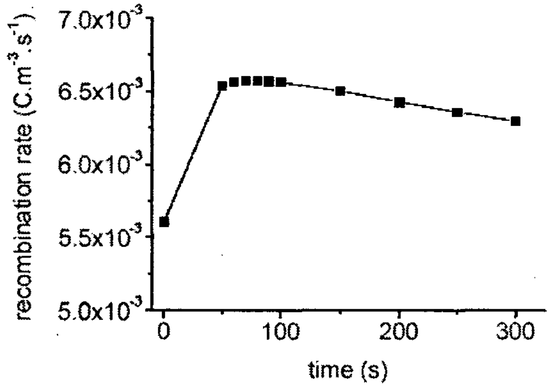

Fig. 6. Time dependence of the recombination rate at differ

Another interesting feature of the current protocol is the memory effect due to the charge stored at a given voltage level on the following one. Figure 7 gives the time dependence of the recombination rate at 10 kV/mm and 40 kV/mm, taking different initial conditions as regards the charge, but going along the same protocol.

Three values of the initial charge density - net zero - have been tested, from 0 to 1 C. m^{-3}. It is striking to note that all the curves at 40 kV/mm are superimposed, whereas the curves at 10 kV/mm exhibit huge differences. The charge stored at each voltage level takes over the initial charge density to control the recombination rate. This was confirmed by simulations run at 60 and 80 kV/mm. To check the validity of the hypothesis, we reproduce in Figure 8 the density of trapped holes (taken as an example - the same would hold for trapped electrons) versus sample thickness at the beginning of the field step at 40, 60 and 80 kV/mm. The density of trapped carriers due to charge storage at a given field level exceeds the initial density introduced at the beginning of the experiment (0.1 C. m^{-3} in this case), thereby confirming the memory effect observed for this protocol.

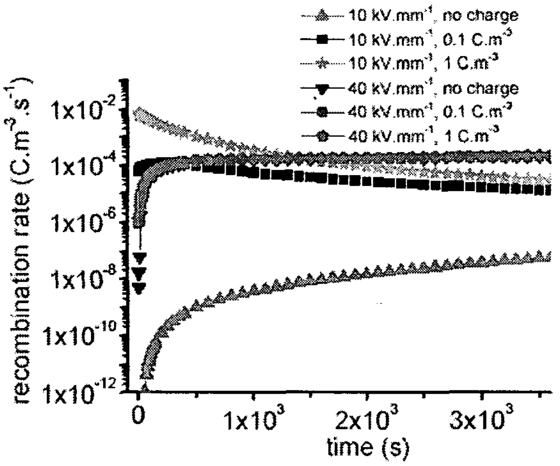

Fig. 6. Time dependence of the recombination rate at 10 and 40 kV/mm for different initial charge density (net zero), keeping the same protocol for voltage application.

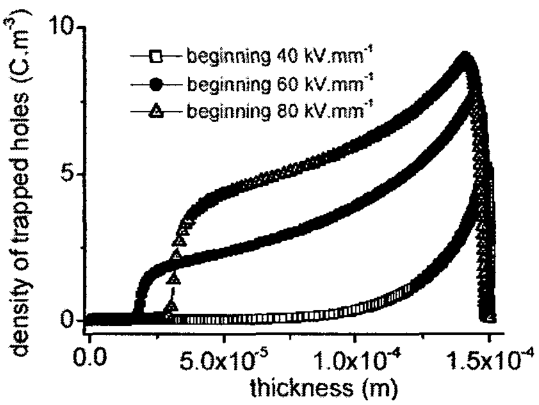

Fig. 7. Trapped holes distribution at the beginning of the application of 40, 60 and 80 kV/mm field (initial charge density is 0.1 $C.m^{-3}$ at 10 kV/mm). The trapped charge exceeds the initial charge density that takes over in controlling the recombination rate.

4. Conclusion

In this paragraph, the main results are summarized, the discrepancies are discussed and we put forward some future work.

1. There is a strong consistency between

experimental observations and model output as regards field and time dependence of the EL. More than phenomenological, the model can be said semiquantitative. It provides evidence that charge recombination is a central process in EL excitation in polyethylene.

2. The existence of a threshold in time for the observation of the EL under constant stress is selfcontained in the hypotheses of the model. However, it has never been clearly observed. This can be explained by several factors. The first one is the possible existence of a distribution of charge in any dielectric before voltage application, but with characteristics that make their detection impossible using space charge detection technique. This could be the case for a distribution of charge with density below the detectable level (sensitivity limit of 10^{-1} C.m^{-3}), or with a higher density of charges, but having a net zero density (any space charge detection set-up probes only the net charge). We have used the hypothesis of a uniform distribution of zero net charge density in the simulation, and we have shown that the threshold in time is effectively "smeared out". The second factor could be the contribution of hot carriers to the EL at very short time in certain circumstances.
3. Shape of EL transients at short time are influenced by the initial charge distribution, being introduced arbitrarily or being due to the charge stored during previous voltage application. In any case, it is not possible to simulate the transient EL observed at short time upon voltage application. There is always either a continuous increase or a peak in the simulated recombination rate, unlike in experiments.

감사의 글

이 논문은 산업자원부에서 시행하는 전력산업 기초인력양성사업 (I-2006-0-092-01)에 의해 작성되었습니다.

[References]

[1] See for example J. J. O'Dwyer, "The theory of electrical conduction and breakdown in solid dielectrics", Clarendon Press, Oxford, UK, 1973.

[2] M. Nagao, T. Kitamura, Y. Mizuno, M. Kosaki and M. Ieda, "Localized heat generation before dielectric breakdown of polyethylene films", International Conference on Conduction and Breakdown of Solid Dielectrics (ICSD), pp. 77-81, July 3-6, 1989, Trondheim, Norway.

[3] C. Laurent, "Optical Pre-Breakdown Warnings in Insulating Polymers", IEEE Magazine EI, Vol. 15, N°2, pp. 5-13, March/April 1999.

[4] L. Sanche, "Electronic aging and related electron interactions in thin-film dielectrics", IEEE Trans. on EI, Vol. 28, pp. 789-819, 1993.

[5] G. Teyssedre, C. Laurent, G. C. Montanari, F. Palmieri, A. See, J. C. Fothergill and L. Dissado, "Charge Distribution and Electroluminescence in XLPE under DC field", J. Phys. D: Appl. Phys., Vol. 34, pp.2830-2844, 2001.